



Contents lists available at ScienceDirect

Environmental Pollution

journal homepage: www.elsevier.com/locate/envpol

The role of different functional groups in a novel adsorption-complexation-reduction multi-step kinetic model for hexavalent chromium retention by undissolved humic acid[☆]

Jia Zhang, Huilin Yin, Linpeng Chen, Fei Liu^{*}, Honghan Chen

Beijing Key Laboratory of Water Resources & Environmental Engineering, China University of Geosciences, Beijing 100083, China

ARTICLE INFO

Article history:

Received 5 August 2017

Received in revised form

22 September 2017

Accepted 28 October 2017

Available online xxx

Keywords:

Humic acid

Hexavalent chromium

Functional groups

Multi-step kinetic model

2DCOS

ABSTRACT

Undissolved humic acid (HA) has a great retention effect on the migration of hexavalent chromium [Cr(VI)] in soil, and HA functional groups play a predominant role in this process. However, the coupled mode between Cr(VI) retention and HA functional groups reaction is still unclear. In this study, it was found that a fair amount of Cr on HA existed in the forms of ion exchangeable and binding Cr(VI) during the reaction resulting from the ion exchange adsorption and complexation of Cr(VI). According to the results of two-dimensional correlation spectroscopic analysis (2DCOS), HA functional groups participated in the reaction with Cr(VI) in the order of carboxyl \approx chelated carboxyl > phenol > polysaccharide > methyl, and all the functional groups were more likely to be located at aromatic domains. Based on the results of XPS spectra, rather than to be oxidized by Cr(VI), carboxyl more tended to be complexed by chromium, which is regarded as the precondition for Cr(VI) reduction. Phenol, polysaccharide and methyl with distinct reaction activities successively acted as major electron donors for Cr(VI) reduction in different reaction stages. Consequently, it was determined that the retention of Cr(VI) by undissolved HA followed an adsorption-complexation-reduction mechanism, and based on this, a multi-step kinetic model with multiple types of complexation/reduction sites was developed to simulate the retention processes resulting in a much better fitting effect ($R^2 > 0.99$) compared with traditional first-order and second-order kinetic models ($R^2 < 0.95$). This demonstrated that the multi-step kinetic model is of great potential in accurately simulating the migration and transformation of Cr(VI) in soil environment.

© 2017 Published by Elsevier Ltd.

1. Introduction

Hexavalent chromium [Cr(VI)] is one of the most common heavy metal pollutants in groundwater, which is of great scientific concern due to its high mobility and acute toxicity to human (Brose and James, 2013). Rather than natural occurrence of Cr(VI) in the stratum (Landrot et al., 2012a,b; Rajapaksha et al., 2013), the main source of Cr(VI) in groundwater is the infiltration of Cr(VI) containing sewages from the anthropogenic activities on the ground, such as electroplating, leather tanning, dyeing, and metallurgy (Dhal et al., 2013). The soil layer located at the top of vadose zone has significant retention effect on Cr(VI) migration, and the soil

organic matter (SOM), Fe(II), and S(II) are considered as the main electron donors for Cr(VI) reduction to its trivalent form [Cr(III)] that is of much lower mobility and toxicity (Hsu et al., 2009). As known, Fe(II) and S(II) are more readily oxidized to higher valent form compared with SOM under oxic condition of surface soil, and therefore, SOM is considered to be of great importance for Cr(VI) reduction and immobilization (Jardine et al., 2013; Leita et al., 2009).

Humic acid (HA), one of the most abundant SOM constituents, has been widely studied in the reaction with Cr(VI), but the majority of related studies were focused on the HA in the form of dissolved organic matter (DOM) (Chen et al., 2011; Wittbrodt and Palmer, 1996, 1997). It has been reported elsewhere that HA in soil mainly exist in the undissolved form (Klučáková and Kolajová, 2014), the mass content of which is generally about two orders of magnitude greater than that of dissolved HA (DOM) in soil water (Xiao et al., 2012), and the environmental implications of them can

[☆] This paper has been recommended for acceptance by Baoshan Xing.

^{*} Corresponding author. Beijing Key laboratory of Water Resources and Environmental Engineering, China University of Geosciences, Beijing 100083, China.

E-mail address: feiliu@cugb.edu.cn (F. Liu).

be quite different from each other. Weng et al. has reported that the existence of HA (DOM) can even increase the concentration of dissolved metals by more than two orders of magnitude to facilitate the transport of heavy metals in soil (Weng et al., 2002). Undissolved HA, on the other hand, has been taken as a good adsorbent for Cr(VI) removal from water (Arslan et al., 2010; Kyziol et al., 2006; Li et al., 2008), which is considered to be in favor of Cr(VI) immobilization. Compared with dissolved HA, undissolved HA therefore tends to play a predominant role for Cr(VI) retention in soil, either from the perspective of quantity or property.

The pathway for Cr(VI) retention by undissolved HA is complicated involving the processes of adsorption, reduction, and complexation (Janos et al., 2009), the understanding of which is of great significance both for the prediction of Cr(VI) fate in the environment and the assessment of Cr(VI) risk for humans. However, the detailed mechanism is still unclear at present. HA functional groups are widely considered to be of vital importance in reaction processes with Cr(VI) by acting as both electron donors and complexation sites (Ohta et al., 2012). Among all the processes, the reduction of Cr(VI) by functional groups get the most scientific concerns, because it will reduce the toxicity and mobility of chromium. Carboxyl and phenol have been reported to be mainly responsible for the reduction of Cr(VI) according to infrared spectroscopy evidence (Huang et al., 2012; Zhao et al., 2016). From the point of view of classical organic chemistry, however, carboxyl is not a representative reducing functional group, and it can only be oxidized though decarboxylation producing carbon dioxide (Brose and James, 2013), which is much more difficult to happen than the oxidation of phenol, hydroxyl, and even methyl groups. Since multi process being involved in the reaction, will there be a possibility that instead of oxidation by Cr(VI) the decreasing infrared absorbance of carboxyl is induced by another process, such as complexation of chromium? In other words, what will be the coupled mode between Cr(VI) retention processes and HA functional groups reaction? This question is of vital importance for the interpretation and prediction of the mechanism and processes for Cr(VI) retention by HA functional groups, however, it has not been fully resolved.

In this work, the retention process of Cr(VI) by undissolved HA was studied, and the variations of chromium concentration and valence state in both aqueous and solid phase with time were investigated. On the other hand, a series of spectroscopies were utilized to characterize the variations of functional groups in the meantime, and then two-dimensional spectroscopy correlation analysis (2DCOS) was employed to reveal the coupled mode between Cr(VI) retention processes and functional groups reaction, based on which a multi-step kinetic model for Cr(VI) retention by undissolved HA was developed.

2. Materials and methods

2.1. Cr(VI) sorption by HA

Commercial HA (Sinopharm Chemical Reagent Co., China) was sieved through a 74 μm sieve to remove coarse particulates, and homogenized. The element composition, acidic groups content, ash content, water content, surface area, point of zero charge (pH_{PZC}) can be found in our previous work (Zhang et al., 2017).

A series of 250 mL of Cr(VI) solutions with initial concentrations of 5 mM were added into 300 mL brown flasks containing 125.0 ± 0.5 mg HA. The solution contained a background electrolyte of 0.01 M NaCl, and the initial pH was adjusted to 1 by adding 2.5 M HCl. Each solution was shaken at 25 $^{\circ}\text{C}$ using a horizontal shaker with an intensity of agitation of 200 rpm. A control experiment was conducted in the same procedure just without HA. All experiments

were performed in triplicate. At given time intervals, 10 mL of each supernatant was sampled by filtering through a 0.45 μm membrane, and then the vacuum filtration was used to separate undissolved HA from the solutions. One of the three HA samples was freeze-dried for Fourier transform infrared spectroscopy (FTIR), solid-state cross-polarization magic angle spinning ^{13}C nuclear magnetic resonance (^{13}C CP/MAS NMR), X-ray photoelectron spectroscopy (XPS), and scanning electron microscopy/energy dispersive X-ray analysis (SEM-EDX) characterization. The other two samples were sequentially desorbed by 250 mL 0.1 M $\text{Na}_2\text{HPO}_4/\text{KH}_2\text{PO}_4$ and 0.1 M NaOH for 2 d and 1 d respectively, and 10 mL supernatant was filtered through 0.45 μm membrane. The HPO_4^{2-} and H_2PO_4^- with high concentration are considered to be able to desorb nearly all the ion exchangeable Cr(VI) on HA (Kozuh et al., 2000). The HA will be completely dissolved in the high concentration of NaOH, and the binding Cr(VI) that cannot be desorbed by phosphate solution will be released into aqueous phase. The concentration of Cr(VI) in the filtrate was determined using a UV/vis spectrophotometer (SHIMADZU UV-1800) at 540 nm after reacting with 1,5-diphenylcarbazide indicator (DPC). Total chromium was determined using ICP-AES (SPECBLUE) at 283.56 nm. The Cr(III) concentration in the filtrate was determined by the difference between total chromium and Cr(VI) concentration.

2.2. FTIR, ^{13}C CP/MAS NMR, XPS, and SEM-EDX characterization

FTIR spectra of samples were obtained on an IR spectrometer (Bruker LUMOS, Germany) at room temperature. All samples were fully ground to guarantee high homogeneity prior to tests. The samples were uniformly mixed with dried KBr powder at mass ratio of 1:200. Each spectrum was obtained after 64 scans with 2 cm^{-1} resolution.

Solid-state ^{13}C CP/MAS NMR spectra of the samples were collected on a Bruker AVANCE III 400 NMR spectrometer with 4 mm NMR rotors with Kel-F caps. NMR spectra were obtained by applying the following parameters: rotor spin rate of 13 kHz, 1s recycle time, 2 ms contact time, 20 ms acquisition time, and 10000 scans. Chemical shifts were calibrated with adamantane.

XPS was measured with Thermo escalab 250XI. The X-ray excitation was provided by a monochromatic Al K α (excitation energy 1486.6 eV). The binding energies of the spectra were corrected using the hydrocarbon component of adventitious carbon at 284.8 eV.

2.3. 2DCOS analysis

The spectra of a series of HA samples from FTIR and ^{13}C CP/MAS NMR under the perturbation of pH were analyzed by the method described by Noda and Ozaki (2005). The dynamic spectra that represents the variation of spectral intensity compared with the reference spectrum can be calculated from the following:

$$\tilde{x}(v) = \bar{x}(v, t_j) = x(v, t_j) - \bar{x}(v), j = 1, 2, \dots, m \quad (1)$$

where the variable v is the spectral index of FTIR, NMR or XPS. $\bar{x}(v, t_j)$ is the dynamic spectra measured at m equally spaced points in perturbation t between t_1 and t_m , and the average spectrum $\bar{x}(v) = \sum_{j=1}^m x(v, t_j)/m$ has been subtracted from raw data $x(v, t_j)$. The synchronous correlation intensity of two spectral indices can be directly calculated from the following:

$$\Phi(v_1, v_2) = \frac{1}{m-1} \sum_{j=1}^m \tilde{x}_j(v_1) \cdot \tilde{x}_j(v_2) \quad (2)$$

Asynchronous correlation intensity of two spectral indexes can be obtained by:

$$\Psi(v_1, v_2) = \frac{1}{m-1} \sum_{j=1}^m \tilde{x}_j(v_1) \cdot \sum_{k=1}^m N_{jk} \cdot \tilde{x}_k(v_2) \quad (3)$$

where N_{jk} corresponds to the j th column and the k th row element of the discrete Hilbert-Noda transformation matrix, which is defined as follows:

$$N_{jk} = \begin{cases} 0, & \text{if } j = k \\ \frac{1}{\pi(k-j)}, & \text{otherwise} \end{cases} \quad (4)$$

Synchronous correlation spectrum $\Phi(v_1, v_2)$ represents synchronous changes of two spectral intensities measured at v_1 and v_2 . A positive $\Phi(v_1, v_2)$ indicates that the spectral intensities at v_1 and v_2 are either increasing or decreasing simultaneously. A negative value indicates that one of the spectral intensities is increasing while the other is decreasing. The asynchronous correlation spectrum $\Psi(v_1, v_2)$ reflects the sequential order of intensity changes of two spectral intensities measured at v_1 and v_2 . If $\Phi(v_1, v_2)$ and $\Psi(v_1, v_2)$ have the same sign, the change in the spectral intensity at v_1 always occurs prior to that at v_2 . In contrast, the sequential orders are reversed if $\Phi(v_1, v_2)$ and $\Psi(v_1, v_2)$ have the opposite sign, and the changes at v_1 and v_2 occur simultaneously if $\Psi(v_1, v_2)$ is zero.

Prior to 2DCOS analysis, the spectra of FTIR were normalized and denoised by Savitzky-Golay smoothing. The peak fitting of XPS data was conducted on XPSPEAK41 software. The 2DCOS analysis was produced using 2Dshige software (Kwansei-Gakuin University, Japan). The data fitting by the multi-step kinetic model was achieved by 1stOpt 7.0 software.

3. Results and discussion

3.1. Process of Cr(VI) retention by HA

In order to determine Cr(VI) retention process by HA within an acceptable time scale and ensure functional groups making significant responses, excess Cr(VI) was added into the reaction

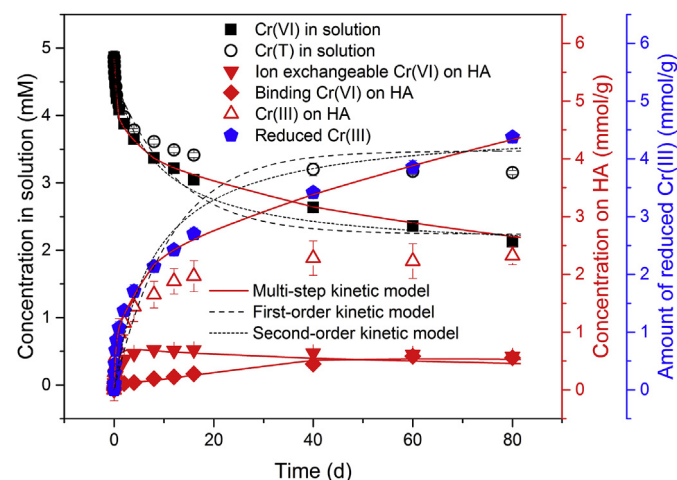


Fig. 1. Concentration variations of Cr with different valent state in solution and on HA with time under initial pH 1 with 125 mg HA in 250 mL solution. No detectable Cr(VI) concentration attenuation was found in the control group without HA as shown in the supplementary materials. Amounts of Cr on HA and reduced Cr(III) are expressed by solid phase concentration, mmol/g. Error bars are SEM ($n = 5$).

system containing HA under pH 1 (the pH almost kept constant throughout the experiment as shown in Fig. S1), and the variations of Cr concentration in solution and on HA with time are shown in Fig. 1. The concentration of Cr(VI) and total Cr [Cr(T)] in solution dropped rapidly during initial period, but the attenuation rate decreased significantly after 8 d. The decreasing of Cr(T) concentration in solution indicated that Cr was adsorbed from aqueous phase onto HA solid phase.

Except for the increasing concentration of reduced Cr(III) on HA with time, a fair amount of Cr existed on HA in the forms of ion exchangeable and binding Cr(VI), which were determined by the method of sequential desorption with 0.1 M $\text{Na}_2\text{HPO}_4/\text{KH}_2\text{PO}_4$ and 0.1 M NaOH. Concentration of ion exchangeable Cr(VI) increased rapidly during initial period, while that of binding Cr(VI) increased slowly with time. This indicated that not all the Cr(VI) adsorbed onto HA tended to be reduced into Cr(III) directly, and the ion exchangeable and binding Cr(VI) may act as intermediates in the reaction processes. Cr(VI) reduction in liquid phase is not considered, because only a slight amount of HA dissolved in solution during the reaction as shown in Fig. S3, which can be almost neglected. The reduced Cr(III) concentration on HA attained a maximum value at about 40 d, and the maximum adsorption capacity of Cr(III) reached as high as 2.56 mmol/g (133.12 mg/g). According to the pH_{PZC} (1.08) of HA, under pH 1 condition the HA surface was positively charged, so Cr(III) cations were not likely to be adsorbed on HA in large quantity by electrostatic attraction. Additionally, under such acidic condition Cr(III) almost cannot exist as hydroxide precipitate either. Therefore, Cr(III) on HA more tended to be complexed by oxygen-containing functional groups, and the maximum adsorption capacity of Cr(III) may be mainly limited by the quantity of complexation sites on HA.

As shown by the blue pentagon points in Fig. 1, which represent the variation of total reduced Cr(III) in the system, the reduction of Cr(VI) was very fast during initial period, but after 16 d the reduction rate dropped significantly to be maintained at a low constant level, reflecting a piecewise feature. Since the complexation sites for Cr(III) had been nearly saturated by 16 d, the reduced Cr(III) afterward was mainly released into aqueous phase resulting in Cr(III) concentration raising in solution. As the concentration of Cr(VI) in solution by the end of experiment was still considerable, the Cr(VI) reduction rate decreasing was more likely due to the quantity limitation of reducing organic functional groups on HA. Additionally, the reasons for piecewise feature of Cr(VI) retention and reduction may be that the high activity organic functional groups were exhausted during the initial period, and at the slow reaction stage mainly the functional groups with low activity took effect.

The variation of Cr valent state distribution on HA with time was further determined by XPS as shown in Fig. 2. As indicated, the absolute intensity of XPS Cr 2p increased with time, which is consistent with the increasing adsorption amount of Cr on HA with time as shown above. The distinct Cr(VI) peaks at 579.3 and 588.6 eV further supports the existence of ion exchangeable and binding Cr(VI) on HA. As shown in Table S1, the percentage of Cr(III) increased from 53.97% at 8 h to 63.22% at 80 d, which further indicated the occurrence of Cr(VI) reduction on HA.

3.2. Role of different HA functional groups

To identify the changes of HA functional groups during reaction with Cr(VI), FTIR was utilized to determine the variations of functional groups with time up to 80 d, and the results are shown in Fig. 3. The absorbance of peaks at 1708, 1249, and 1369 cm^{-1} decreased with time significantly, which are respectively assigned to C=O stretching vibration of carboxyl, C-O stretching vibration of

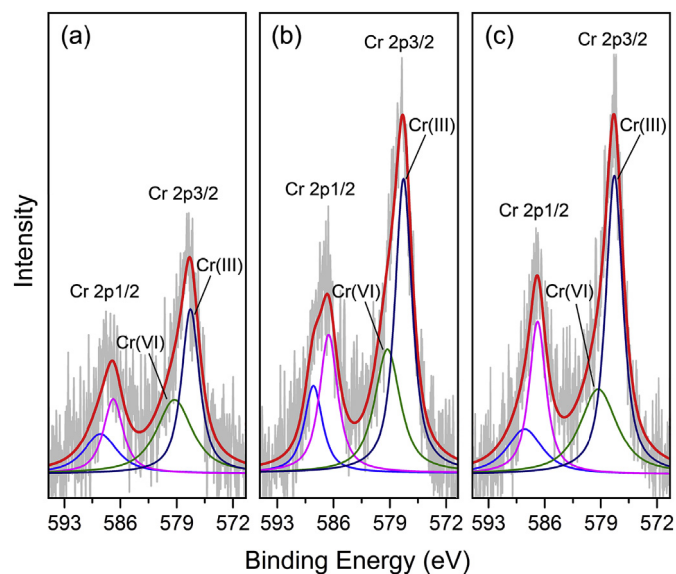


Fig. 2. XPS Cr 2p spectra of HA after reacting with 5 mM Cr(VI) for (a) 8 h, (b) 8 d, and (c) 80 d. The peaks at 577.3 and 586.9 eV binding energy represent Cr(III), and peaks at 579.4 and 588.6 eV binding energy represent Cr(VI). % Lorentzian-Gaussian ratio was fixed at 80. The 2p doublet separation of Cr(III) and Cr(VI) are 9.6 and 9.2 eV respectively. The area ratio of Cr 2p_{1/2} to Cr 2p_{3/2} is 1:2.

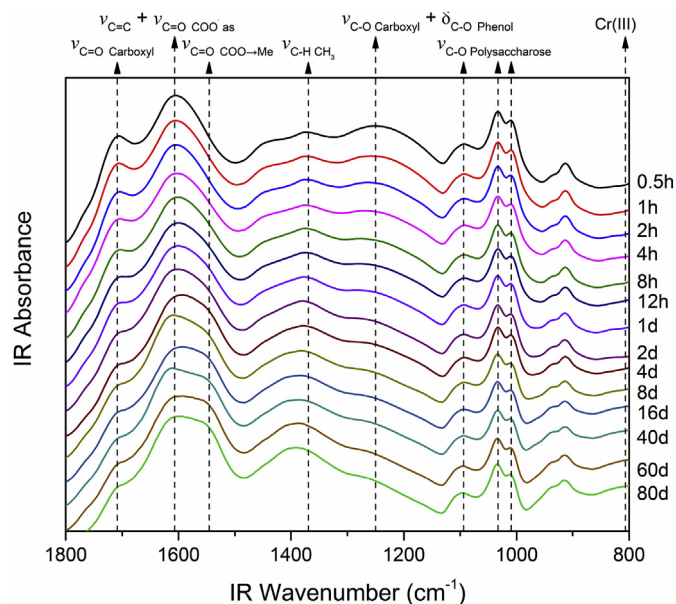


Fig. 3. FTIR absorbance spectra of the freeze-dried HA samples after reacting with Cr(VI) for different time ranging from 0.5 h to 80 d.

phenol, and C-H deformation vibration of methyl (Fanning and Vannice, 1993; Li et al., 2003; O'Reilly and Mosher, 1983; Sellitti et al., 1990). On the contrary, the absorbance of the peaks at 1546 and 804 cm^{-1} increased with time, which can be observed clearly by overlapping peaks resolving as shown in Fig. S4, and they can be attributed to the chelated carboxyl group and Cr(III) respectively (Zhao et al., 2016). The absorbance decreasing of peaks at 1094, 1033, and 1009 cm^{-1} , which are all attributed to C-O stretching vibration of polysaccharide (Chen et al., 2015), was not obvious with the relative shape of peaks nearly remaining unchanged with time. However, considering methylene ($-\text{CH}_2-$) nearly doesn't

participate in the reaction with Cr(VI) resulting in the absorbance of the characteristic peak at 1390 cm^{-1} remaining constant, the relative absorbance attenuation of peaks representing polysaccharide can be narrowly observed. Even so, it is still a challenge to accurately make out all the variations of absorbance on account of the badly overlapped FTIR peaks of HA, and it is more unlikely to verify the absorbance changing orders of related peaks effectively.

Consequently, in order to determine the species and orders of HA functional groups participating in the reaction with Cr(VI), 2DCOS was introduced for FTIR spectra analysis, and the results are shown in Fig. 4. Five predominant auto-peaks can be readily

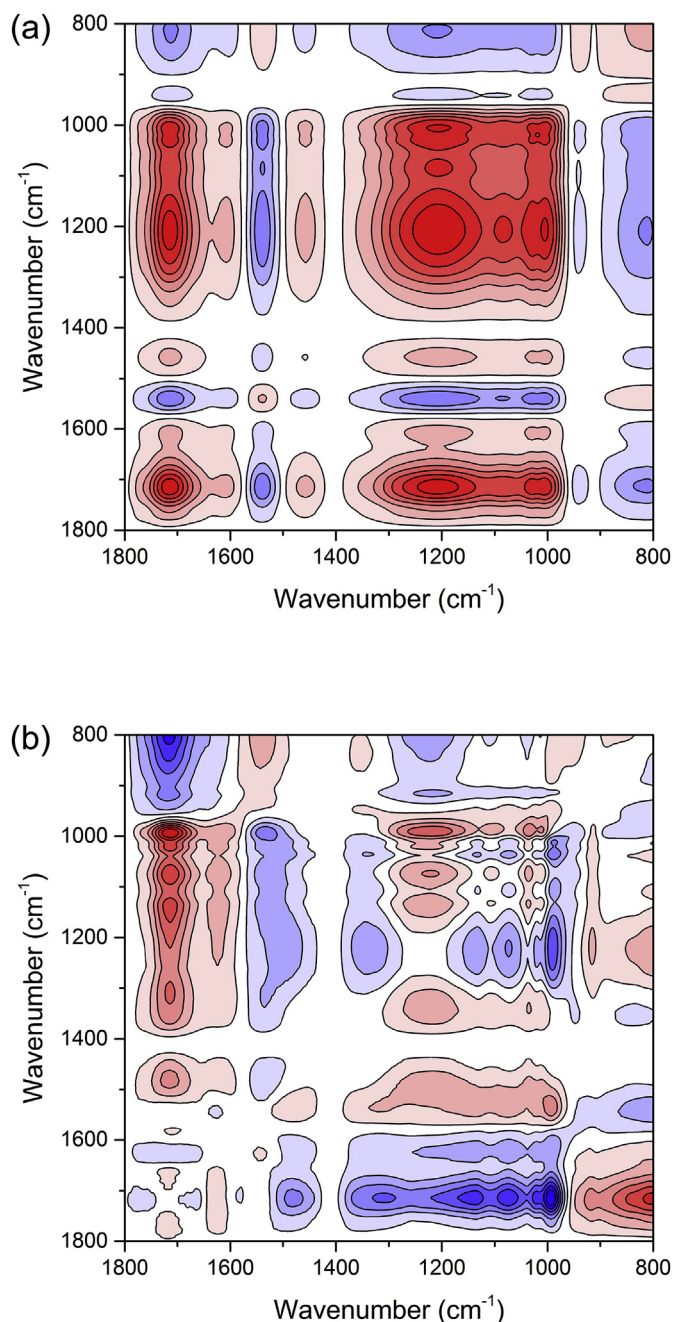


Fig. 4. (a) Synchronous and (b) asynchronous maps of 2DCOS for FTIR spectra obtained from HA samples after reacting with Cr(VI) for different time. Red regions represent the positive correlation intensity; blue regions represent the negative correlation intensity. (For interpretation of the references to colour in this figure legend, the reader is referred to the web version of this article.)

distinguished on the diagonal of synchronous map centered at 1708, 1546, 1249, 1033, and 804 cm^{-1} , and a small peak at 1369 cm^{-1} can be observed in asynchronous map which was covered by peak at 1249 cm^{-1} in synchronous map. This further indicated that mainly free carboxyl, chelated carboxyl, phenol, polysaccharide, and methyl of HA participated in the reaction with Cr(VI). The red (or blue) regions, namely cross-peaks, at upper-left corner of synchronous map indicated the absorbance at corresponding two wavenumbers changed in the same (or opposite) direction (Noda, 1993). It can be concluded that the absorbance of chelated carboxyl (1546 cm^{-1}) and Cr(III) (804 cm^{-1}) changed in opposite directions from the other functional groups, which is consistent with the judgement based on the one-dimensional spectra.

The sign relationship between synchronous and asynchronous map and peak assignment are summarized in Table 1, and according to the rules for changing order determination (Chen et al., 2014), the variation of HA functional groups followed the order: free carboxyl (1708 cm^{-1}) \approx chelated carboxyl (1546 cm^{-1}) > phenol (1249 cm^{-1}) > polysaccharide (1033 cm^{-1}) > methyl (1369 cm^{-1}). According to the results, the FTIR absorbance of free carboxyl and chelated carboxyl changed almost simultaneously in opposite directions, indicating that the FTIR absorbance attenuation of free carboxyl tended to be induced by the complexation of Cr. Additionally, the changing order of phenol, polysaccharide, and methyl was consistent with the knowledge of classical organic chemistry about reducibility of organic functional groups, phenol > polysaccharide (hydroxyl) > methyl, indicating that these functional groups with different reducibility tended to successively act as main electron donors in different reaction stage for Cr(VI) reduction. However, according to classical organic chemistry the reducing capacity of carboxyl is much lower than that of phenol, hydroxyl, and methyl, in other words, it is not likely to be oxidized by Cr(VI) preferentially. Therefore, the carboxyl more tended to be complexed by Cr rather than oxidized by Cr(VI).

To further confirm whether HA carboxyl was oxidized in the reaction with Cr(VI), XPS C 1s was employed to reveal the variations of carbon binding characteristics, and the results are shown in Fig. 5. As indicated, the XPS intensity of C-C and C-H nearly remained unchanged with time, but that of C-O, representing phenol and polysaccharide, decreased significantly with time. By 80 d, there was only trace amount of C-O that could be detected resulting from the oxidation induced by Cr(VI). On the contrary, the intensity of O=C=O, representing carboxyl like groups, almost kept constant throughout the reaction, which further verified that the carboxyl are more likely to form complex with Cr rather than be oxidized by Cr(VI).

Solid-state ^{13}C CP/MAS NMR was utilized to reveal the variations of HA molecular structures during reacting with Cr(VI), and the results were shown in Fig. S5. The intensities at 168, 155, 127, and

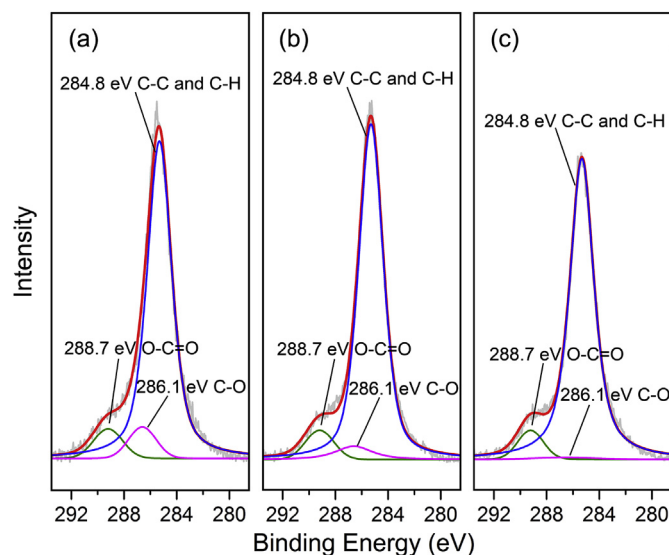


Fig. 5. XPS C 1s spectra of HA after reacting with 5 mM Cr(VI) for (a) 8 h, (b) 8 d, and (c) 80 d.

30 ppm decreased with time, which are attributed to carboxylic C, phenolic C, aromatic C, and alkyl C respectively (Xing, 2001), and the intensity attenuation of aromatic C was most significant. The result of two-dimensional hetero-spectral correlation analysis for FTIR and ^{13}C CP/MAS NMR (Fig. 6) indicated that the HA functional groups participating in the reaction with Cr(VI) were more likely to be located at aromatic domains of HA molecules.

3.3. Mechanism of Cr(VI) retention by HA functional groups

Base on the results above, the mechanism of Cr(VI) retention by HA functional groups was revealed as shown in Fig. 7. According to Stern electrical double-layer theory, liquid film diffusion that takes place in the diffusion layer is inevitable for the Cr(VI) in bulk

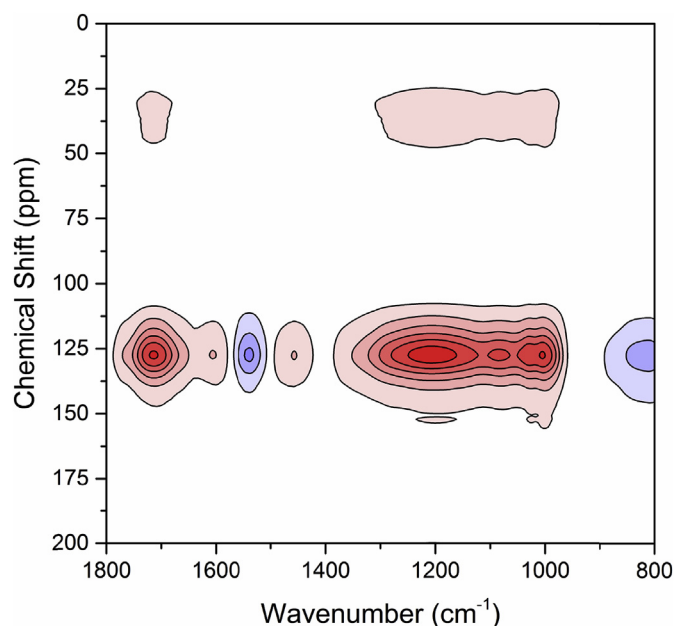


Fig. 6. Synchronous map of two-dimensional hetero-spectral correlation analysis for solid-state ^{13}C CP/MAS NMR and FTIR spectra of HA after reacting with Cr(VI).

Table 1

The peak assignment and sign relationship between synchronous and asynchronous maps of HA after reacting with Cr(VI) for different time.

Position (cm^{-1})	Peak assignment	Sign ^a			
		1708	1546	1369	1249
1708	Carboxyl $\nu_{\text{C=O}}$				
1546	Chelated carboxyl $\nu_{\text{C=O}}$	0			
1369	Methyl $\nu_{\text{C-H}}$	+	+		
1249	Phenol $\nu_{\text{C-O}}$	+	+	-	
1033	Polysaccharide $\nu_{\text{C-O}}$	+	+	-	+

^a Signs were obtained in the upper-left corner of the maps: +, same sign; -, opposite sign; 0, value in asynchronous map is zero.

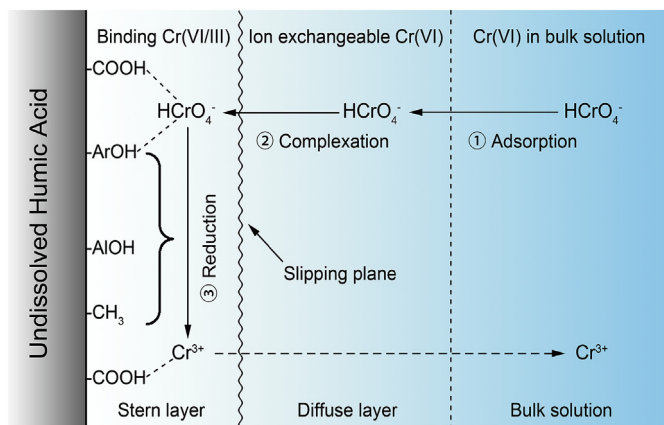


Fig. 7. Proposed scheme of Cr(VI) retention by different functional groups of undissolved HA.

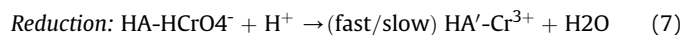
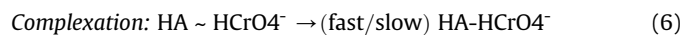
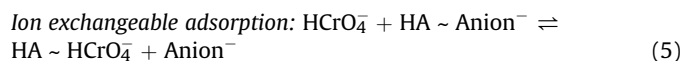
solution transports onto HA surface. As the diffusion layer is positive charged under the experimental condition, a certain amount of Cr(VI) anions will be kept in the diffusion layer by electrostatic attraction in the form of ion exchangeable Cr(VI), which won't be reduced because of the isolation from the electron donors of functional groups on HA surface. When Cr(VI) in the diffusion layer transports into the Stern layer, the formation of corresponding complexation between Cr(VI) and functional groups on HA surface will take place resulting in the occurrence of binding Cr(VI) on HA as observed above. The binding Cr(VI), as an intermediate, will be consequently reduced to Cr(III) by adjacent functional groups (phenol, hydroxyl, and methyl) with different reducibility.

Even though it has been reported that Cr(VI) anion can form complex with low molecular weight organic matters by forming chromate ester with various functional groups, such as carboxyl, phenol, hydroxyl and thiol (Brose and James, 2013; Hasan and Rocek, 1973), the complexation mechanism with HA functional groups is still unknown resulting from the high heterogeneity of HA functional groups. Elovitz and Fish reported that the formation of Cr(VI)-phenol complex through chromate ester is the precursor for Cr(VI) reduction by substituted phenols, and the reaction rate constants vary with substituent groups (Elovitz and Fish, 1995). This means that even for a single functional group the reactivity may be various for Cr(VI) complexation and reduction induced by the difference on substitution environment, and it will become more random for HA functional groups with more complicated substitutions. Additionally, considering that it has been reported before that multiple functional groups may be involved for single Cr(VI) anion complexation (Brose and James, 2013), therefore, it is nearly impossible at present to accurately indicate the types, coordination environment and activity of functional groups participating in Cr(VI) complexation and reduction. However, it can be assumed that various types of complexation/reduction sites exist on HA surface, which respectively consist of one or multiple functional groups for the complexation and reduction of single Cr(VI) anion, and they can be classified into phenol-containing, hydroxyl-containing and methyl-containing complexation/reduction sites with quite different complexation/reduction activities according to the results of 2DCOS analysis.

3.4. Multi-step kinetic model for Cr(VI) retention by HA

The traditional first-order and second-order kinetic model were utilized for the data fitting of Cr(VI) concentration variation in solution and reduced amount of Cr(III) variation in the reaction

system with time as shown in Fig. 1. However, it can be seen that neither of the first-order or second-order kinetic model can describe the reaction process well ($R^2 < 0.95$). The reason for that is the reactions between Cr(VI) and HA involve multiple processes as mentioned above, including ion exchange adsorption, complexation, and reduction of Cr(VI), and thus the retention of Cr(VI) by HA cannot be simply taken as a single step reaction. Therefore, a multi-step reaction model for Cr(VI) retention by HA was proposed as follows according to the reaction mechanism:



where HCrO_4^- represents Cr(VI) in solution; $\text{HA} \sim \text{HCrO}_4^-$ represents ion exchangeable Cr(VI); $\text{HA} \sim \text{HCrO}_4^-$ represents binding Cr(VI). The reaction rate of complexation and reduction of Cr(VI) are differentiated to be fast and slow, because HA functional groups with diverse reaction activities take predominant effect in different reaction stages.

Based on the reaction model, a novel multi-step kinetic model was developed under four simplification assumptions: (1) The ion exchangeable capacity won't change during the adsorption; (2) the complexation of Cr(VI) is the precondition for its reduction; (3) the oxidized complexation/reduction sites lose the ability to complex Cr(VI) again; (4) the attenuations of complexation/reduction sites and complexed sites both follow first-order kinetics. The detailed conceptual model establishment and mathematical deduction procedures can be found in the supplementary materials and the mathematic model is shown as follows:

$$\begin{cases} \frac{dC_1}{dt} = -k_0 \left(C_1 - \frac{\bar{C}_2}{K_d} \right) \\ \frac{d\bar{C}_2}{dt} = -\sum_{i=1}^n k_i \bar{C}_2 q_i e^{-a_i t} + \frac{V}{m} k_0 \left(C_1 - \frac{\bar{C}_2}{K_d} \right) \\ \frac{d\bar{C}_3}{dt} = -\sum_{i=1}^n k_{i+n} \bar{C}_3 q_i (1 - e^{-a_i t}) e^{-b_i t} + \sum_{i=1}^n k_i \bar{C}_2 q_i e^{-a_i t} \\ \frac{d\bar{C}_4}{dt} = \sum_{i=1}^n k_{i+n} \bar{C}_3 q_i (1 - e^{-a_i t}) e^{-b_i t} \end{cases} \quad (8)$$

where C_1 , \bar{C}_2 , \bar{C}_3 , and \bar{C}_4 respectively represent the concentration of Cr(VI) in solution, ion exchangeable Cr(VI) on HA, binding Cr(VI) on HA, and reduced Cr(III) in the reaction system. n is the sum of complexation/reduction sites, and i represents the kinds of complexation/reduction sites. k is the reaction rate constant for Cr(VI). K_d is the equilibrium constant of adsorption reaction. q represents the initial amount of complexation/reduction sites. a and b represent the attenuation rate constant for complexation/reduction sites and complexed sites respectively. V and m are the solution volume of reaction system and mass of HA respectively.

It was assumed that there are three different types of complexation/reduction sites existing on HA ($n = 3$) according to the FTIR results, namely phenol, polysaccharide, and methyl, and the fitting results are shown by the red lines in Fig. 1. As indicated, the multi-step kinetic model fits the Cr(VI) concentration in solution and reduced Cr(III) in the reaction system data quite well ($R^2 > 0.99$), and the ion exchangeable and binding Cr(VI) can also be involved in the new model. The multi-step kinetic model with two

different types of complexation/reduction sites ($n = 2$, phenol and polysaccharide functional groups were used) can also fit the experimental data well ($R^2 > 0.99$), but the fitting effect for binding Cr(VI) is not as good as the model with three different types of complexation/reduction sites. The detailed fitting parameters are shown in Table S2.

4. Conclusion

In this work, a novel adsorption-complexation-reduction multi-step kinetic model was developed based on the retention mechanism of Cr(VI) by undissolved HA, and the role of HA functional groups was taken into consideration. The good performance of the model demonstrated that it is of great potential in application of Cr(VI) migration and transformation simulation in soil, which will further benefit the understanding of Cr(VI) fate in the environment and the assessment of Cr(VI) contaminated soil risk for humans. However, for the reason of determining the Cr(VI) retention process in an acceptable time scale and to make the functional groups give significant responses, the experiment was conducted under a relative low pH, which limits the direct application of the model in the neutral environment, but the extreme acidic contamination condition containing Cr(VI) is also common in real situations, such as electroplating contaminated sites. Nevertheless, to further verify the mechanism under near-neutral conditions is still of great value to make the model more reliable, and this may be the next move of effort direction.

Acknowledgements

This work was financially supported by the National Natural Science Foundation of China (Grant 41672239) and China Geological Survey (1212011121173).

Appendix A. Supplementary data

Supplementary data related to this article can be found at <https://doi.org/10.1016/j.envpol.2017.10.120>.

References

- Arslan, G., Edebali, S., Pehlivan, E., 2010. Physical and chemical factors affecting the adsorption of Cr(VI) via humic acids extracted from brown coals. *Desalination* 255, 117–123.
- Brose, D.A., James, B.R., 2013. Hexavalent chromium reduction by tartaric acid and isopropyl alcohol in mid-atlantic soils and the role of Mn(III,IV)(hydr)oxides. *Environ. Sci. Technol.* 47, 12985–12991.
- Chen, S.Y., Huang, S.W., Chiang, P.N., Liu, J.C., Kuan, W.H., Huang, J.H., Hung, J.T., Tzou, Y.M., Chen, C.C., Wang, M.K., 2011. Influence of chemical compositions and molecular weights of humic acids on Cr(VI) photo-reduction. *J. Hazard Mater* 197, 337–344.
- Chen, W., Qian, C., Liu, X.Y., Yu, H.Q., 2014. Two-dimensional correlation spectroscopic analysis on the interaction between humic acids and TiO₂ nanoparticles. *Environ. Sci. Technol.* 48, 11119–11126.
- Chen, W., Habibul, N., Liu, X.Y., Sheng, G.P., Yu, H.Q., 2015. FTIR and synchronous fluorescence heterospectral two-dimensional correlation analyses on the binding characteristics of copper onto dissolved organic matter. *Environ. Sci. Technol.* 49, 2052–2058.
- Dhal, B., Thatoi, H.N., Das, N.N., Pandey, B.D., 2013. Chemical and microbial remediation of hexavalent chromium from contaminated soil and mining/metal-lurgical solid waste: a review. *J. Hazard Mater* 250–251, 272–291.
- Elovitz, M.S., Fish, W., 1995. Redox interactions of Cr(VI) and substituted phenols: products and mechanism. *Environ. Sci. Technol.* 29, 1933–1943.
- Fanning, P.E., Vannice, M.A., 1993. A DRIFTS study of the formation of surface groups on carbon by oxidation. *Carbon* 31, 721–730.
- Hasan, F., Rocek, J., 1973. Three-electron oxidations. IV. Chromic acid cooxidation of tertiary hydroxy acids and alcohols. *J. Am. Chem. Soc.* 95, 417–429.
- Hsu, N.H., Wang, S.L., Lin, Y.C., Sheng, G.D., Lee, J.F., 2009. Reduction of Cr(VI) by crop-residue-derived black carbon. *Environ. Sci. Technol.* 43, 8801–8806.
- Huang, S.W., Chiang, P.N., Liu, J.C., Hung, J.T., Kuan, W.H., Tzou, Y.M., Wang, S.L., Huang, J.H., Chen, C.C., Wang, M.K., 2012. Chromate reduction on humic acid derived from a peat soil – exploration of the activated sites on HAs for chromate removal. *Chemosphere* 87, 587–594.
- Janoš, P., Hůla, V., Bradnová, P., Pilařová, V., Šedlbauer, J., 2009. Reduction and immobilization of hexavalent chromium with coal- and humate-based sorbents. *Chemosphere* 75, 732–738.
- Jardine, P.M., Stewart, M.A., Barnett, M.O., Basta, N.T., Brooks, S.C., Fendorf, S., Mehlhorn, T.L., 2013. Influence of soil geochemical and physical properties on chromium(VI) sorption and bioaccessibility. *Environ. Sci. Technol.* 47, 11241.
- Ključáková, M., Kolajová, R., 2014. Dissociation ability of humic acids: spectroscopic determination of p K a and comparison with multi-step mechanism. *React. Funct. Polym.* 78, 1–6.
- Kožuh, N., Štupar, J., Gorenc, B., 2000. Reduction and oxidation processes of chromium in soils. *Environ. Sci. Technol.* 34, 112–119.
- Kyzioł, J., Twardowska, I., Schmittkopplin, P., 2006. The role of humic substances in chromium sorption onto natural organic matter (peat). *Chemosphere* 63, 1974–1982.
- Landrot, G., Ginder-Vogel, M., Livi, K., Fitts, J.P., Sparks, D.L., 2012a. Chromium(III) oxidation by three poorly-crystalline manganese(IV) oxides. 1. Chromium(III)-oxidizing capacity. *Environ. Sci. Technol.* 46, 11594–11600.
- Landrot, G., Ginder-Vogel, M., Livi, K., Fitts, J.P., Sparks, D.L., 2012b. Chromium(III) oxidation by three poorly crystalline manganese(IV) oxides. 2. Solid phase analyses. *Environ. Sci. Technol.* 46, 11601–11609.
- Leita, L., Margon, A., Pastrello, A., Arcon, I., Contin, M., Mosetti, D., 2009. Soil humic acids may favour the persistence of hexavalent chromium in soil. *Environ. Pollut.* 157, 1862–1866.
- Li, L., Huang, W., Peng, P.A., Sheng, G., Fu, J., 2003. Chemical and molecular heterogeneity of humic acids repetitively extracted from a peat. *Soil Sci. Soc. Am. J.* 67, 740–746.
- Li, Y., Yue, Q., Gao, B., Li, Q., Li, C., 2008. Adsorption thermodynamic and kinetic studies of dissolved chromium onto humic acids. *Colloids Surf. B* 65, 25.
- Noda, I., 1993. Generalized two-dimensional correlation method applicable to infrared, raman, and other types of spectroscopy. *Appl. Spectrosc.* 47, 1329–1336.
- Noda, I., Ozaki, Y., 2005. Two-dimensional Correlation Spectroscopy: Applications in Vibrational and Optical Spectroscopy. John Wiley & Sons.
- O'Reilly, J.M., Mosher, R.A., 1983. Functional groups in carbon black by FTIR spectroscopy. *Carbon* 21, 47–51.
- Ohta, A., Kagi, H., Tsuno, H., Nomura, M., Okai, T., 2012. Speciation study of Cr(VI/III) reacting with humic substances and determination of local structure of Cr binding humic substances using XAFS spectroscopy. *Geochem. J.* 46, 409–420.
- Rajapaksha, A.U., Vithanage, M., Ok, Y.S., Oze, C., 2013. Cr(VI) Formation related to Cr(III)-muscovite and birnessite interactions in ultramafic environments. *Environ. Sci. Technol.* 47, 9722–9729.
- Sellitti, C., Koenig, J.L., Ishida, H., 1990. Surface characterization of graphitized carbon-fibers by attenuated total reflection fourier-transform infrared-spectroscopy. *Carbon* 28, 221–228.
- Weng, L., Temminghoff, E.J., Lofts, S., Tipping, E., Van Riemsdijk, W.H., 2002. Complexation with dissolved organic matter and solubility control of heavy metals in a sandy soil. *Environ. Sci. Technol.* 36, 4804–4810.
- Wittbrodt, P.R., Palmer, C.D., 1996. Effect of temperature, ionic strength, background electrolytes, and Fe(III) on the reduction of hexavalent chromium by soil humic substances. *Environ. Sci. Technol.* 30, 2470–2477.
- Wittbrodt, P.R., Palmer, C.D., 1997. Reduction of Cr(VI) by soil humic acids. *Eur. J. Soil Sci.* 48, 151–162.
- Xiao, W., Zhang, Y., Li, T., Chen, B., Wang, H., He, Z., Yang, X., 2012. Reduction kinetics of hexavalent chromium in soils and its correlation with soil properties. *J. Environ. Qual.* 41, 1452–1458.
- Xing, B., 2001. Sorption of naphthalene and phenanthrene by soil humic acids. *Environ. Pollut.* 111, 303.
- Zhang, J., Chen, L., Yin, H., Jin, S., Liu, F., Chen, H., 2017. Mechanism study of humic acid functional groups for Cr(VI) retention: two-dimensional FTIR and ¹³C CP/MAS NMR correlation spectroscopic analysis. *Environ. Pollut.* 86–92.
- Zhao, T.T., Ge, W.Z., Nie, Y.X., Wang, Y.X., Zeng, F.G., Qiao, Y., 2016. Highly efficient detoxification of Cr(VI) by brown coal and kerogen: process and structure studies. *Fuel Process. Technol.* 150, 71–77.